

# A New Algorithm for Optical Photomask CD Metrology for the 100-nm Node

Nicholas G. Doe, Richard D. Eandi, Patrick St. Cin  
(Zygo Corporation, 456 Oakmead Parkway, Sunnyvale CA, 94085)

## ABSTRACT

Manufacturing devices at the 100nm node presents new problems for the photomask metrologist. The metrologist is required to measure dense features with arbitrary line and space widths. While existing optical metrology tools are very successful at measuring isolated features with very high precision and repeatability, the conventional threshold algorithms exhibit Optical Proximity Effects (OPE) that affect the accuracy of CD measurements of both isolated and dense features.

This paper presents a new CD metrology algorithm that is highly linear and largely insensitive to the influence of OPE while maintaining high precision and repeatability. The algorithm has been implemented on the new 244nm DUV optical metrology tool, the KMS-100.

Demonstrated performance for the new algorithm on the DUV tool on binary masks shows better than 1.5nm, 3 sigma static repeatability down to 0.25um. Linearity, without multipoint calibration, is better than 5nm down to 0.25um for isolated lines. The OPE sensitivity (difference between measurements of isolated, dense and half isolated lines) for mask features down to 0.4um has been demonstrated to be better than 5nm over a wide range of dense lines and spaces widths.

Keywords: CD metrology, photomask, optical proximity, optical metrology.

## 1. INTRODUCTION

CD metrology using optical microscopy has traditionally used a threshold algorithm whereby the position of an edge is determined by the point at which the intensity crosses a set threshold. The threshold can be based on preset value or by the range of values in the image local to the feature being measured. The local minimum and maximum or "average minimum" and "average maximum" can be used to determine the threshold. For an incoherent<sup>1</sup> imaging system a threshold of 50% should give zero bias between the CD measurements and the feature size. In reality, however, a bias is used to correct the measurements determined by measuring features of a known size. For a coherent imaging system, such as a confocal microscope<sup>2</sup>, the correct threshold is 25% although 50% is typically used for the best noise performance and hence best 3 $\sigma$  static repeatability and a bias applied. Whereas the threshold algorithm has been used very successfully, it is non-linear for small features and suffers from significant optical proximity effects (OPE)<sup>3</sup>. The non-linearity can be measured and corrected using multi-point calibration techniques however similar corrections for OPE are not practical.

Other algorithms have been suggested and used successfully including maximum gradient<sup>3</sup>, peak to peak and flux area<sup>4</sup>. This paper introduces a new algorithm that makes use of a model of the imaging properties of the microscope to refine the calculation of the edge position calculation.

The goals for the new algorithm include:

- Excellent repeatability – comparable to the threshold algorithm.
- Good linearity down to 0.25 $\mu$ .
- Good OPE performance down to 0.35 $\mu$ .
- Insensitive to illumination artifacts including field uniformity and short and long term illumination fluctuations
- Adaptable to different mask types including attenuated PSM, strong PSM and ADI (resist) masks.

## 2. OPE ALGORITHM

The steps in the line width metrology algorithm are:

1. Acquire the microscope image.
2. Locate the approximate position of the edges of the feature and adjacent features.
3. Determine the position of each line edge with high precision.
4. Calculate the feature width as the difference between the edge positions.

It is step 3 which we describe in detail below.

The algorithm makes use of a model of the imaging system. The model is implemented as family of intensity profiles for spaces and lines as shown in figure 1 (spaces only are shown). There are various ways the intensity profile data can be generated:

1. Full theoretical analysis of the imaging system.
2. Experimental characterization of the imaging system and calculation of the profiles.
3. Image capture of known line widths.

For this paper we use the 2<sup>nd</sup> method where the Modulation Transfer Function (MTF) of the system is measured using pair of edges and the image profiles are calculated based on the MTF, this is described in ref 3.

To locate the position of an edge, the new algorithm performs the following steps (expansion of step 3 above):

1. Locate the position of the edge and the adjacent leading and trailing edges (if any) to low accuracy using any standard technique (threshold, maximum gradient etc.).
2. Using the locations of the adjacent edges and the model, refine the calculation for the position of the edge and the adjacent edge(s). Note that the OPE causes the edge shape to change as adjacent edge(s) approach within a wavelength of light of the edge of interest.
3. Iterate step 2 as required using the revised edge positions.

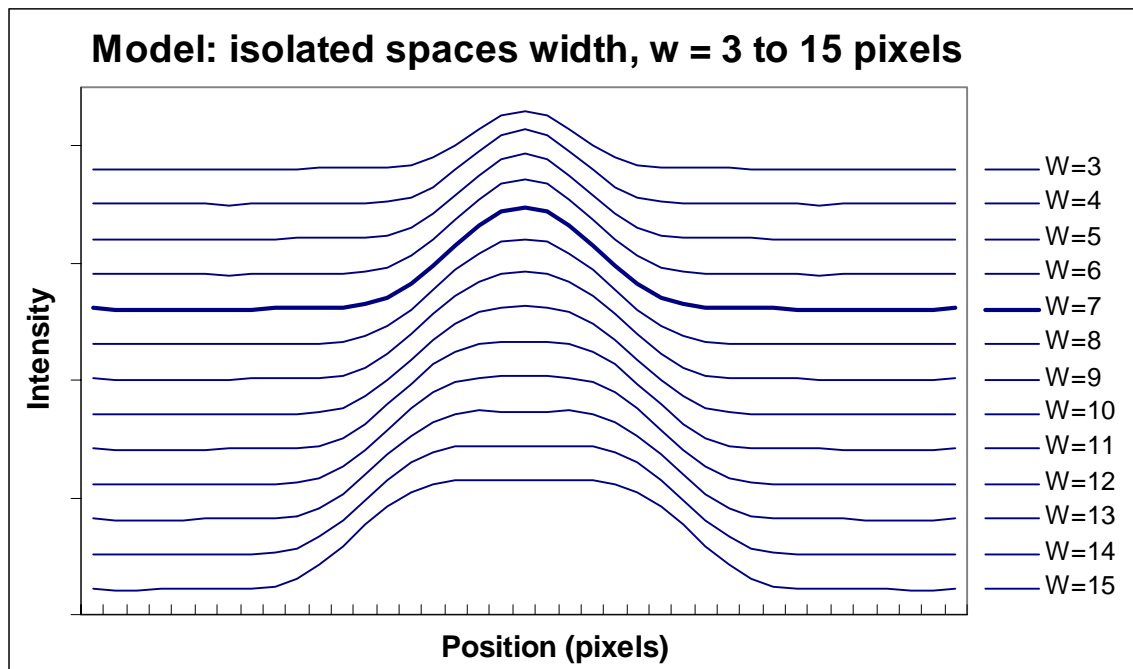


Figure 1. The model consist of intensity profiles for isolated spaces and lines, a limited set of the spaces are shown.

### 2.1 Detailed Description

The new algorithm will be described with reference to an isolated space and then to the more general case of the left line of a line/space array. The model is illustrated in figure 1 and consists of a number of

intensity profiles for different width lines and spaces. For clarity, only a subset of the spaces is shown, the profile for a 7 pixel width space ( $w=7$ ) is highlighted (in the KMS metrology systems, 1 pixel is about 33nm so this corresponds to a 231nm space). The algorithm matches the edges of the model profile with the acquired intensity profile from the reticle; figure 2 shows the left and right edges for the for  $w=7$  profile.

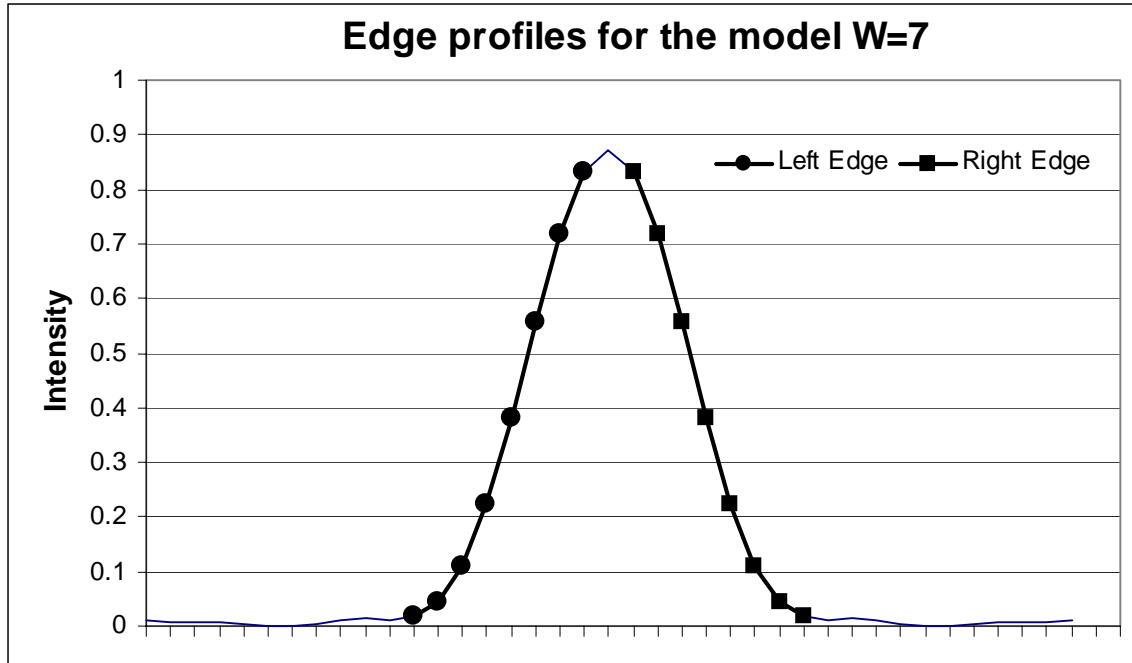


Figure 2. Left and right edge profiles for an isolated space 7 pixels wide.

## 2.2 Isolated Space Measurement

For an isolated line or space, the image profile of an edge changes due to the adjacent edge so the CD non-linearity for isolated features is actually an OPE. To determine the positions of the edges, we compare the acquired image profile with a number of the line widths in the model and interpolate between line widths to get the true position.

Figure 3 is the GUI display for an isolated cross measurement where the top arm of the cross is being measured; the intensity profile for the measurement is seen below the image. Figure 4 shows the magnified intensity profile. We use the threshold algorithm to get the approximate edge positions and line width, the edges are found at pixel 20.37 and pixel 28.25 and the width is 7.88 pixels. The line is about 8 pixels wide, so we will use profiles for line widths 6 through 9 pixels ( $w=6$  to  $w=9$ ) to determine the edge positions and hence the line width. To find the position of the edge (for a given width), we “slide” the model over the image profile and look for the best fit. The approximate position for the left edge is at pixel 20.4 so we slide the model from pixel 18 to pixel 23 as shown in figure 5. The error between the model and the profile is calculated, allowing the model amplitude and offset to change to best match the profile – this allows the algorithm to be immune to variations in illumination across the field of view and over time and immune to video gain and offset (brightness and contrast). Figure 5 inset shows the error as we slide the profile along the image, we get a best match when the edge is at pixel 20.71. To find the position of right edge, we slide the model of the right edge over the profile. For  $w=7$ , the edge position is at pixel 28.11.

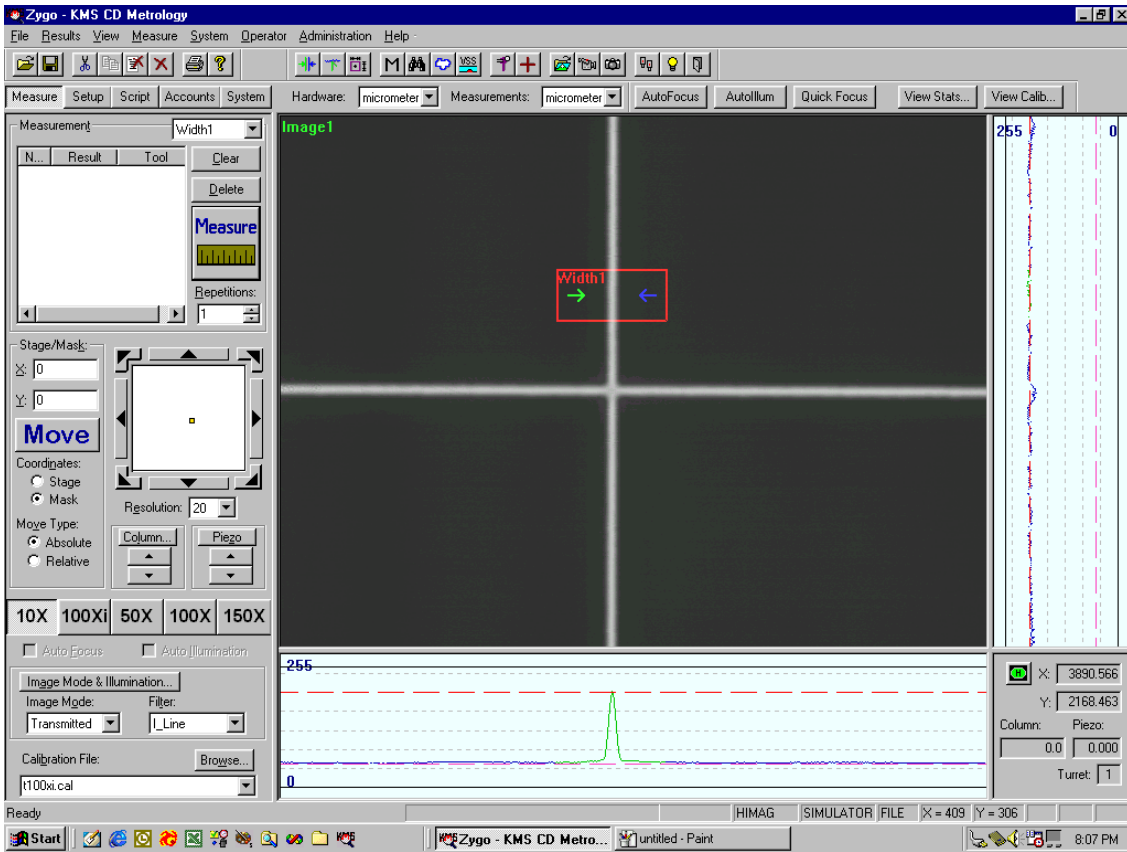


Figure 3. GUI display for the measurement of an isolated cross (isolated space), note the intensity profile is shown below the image.

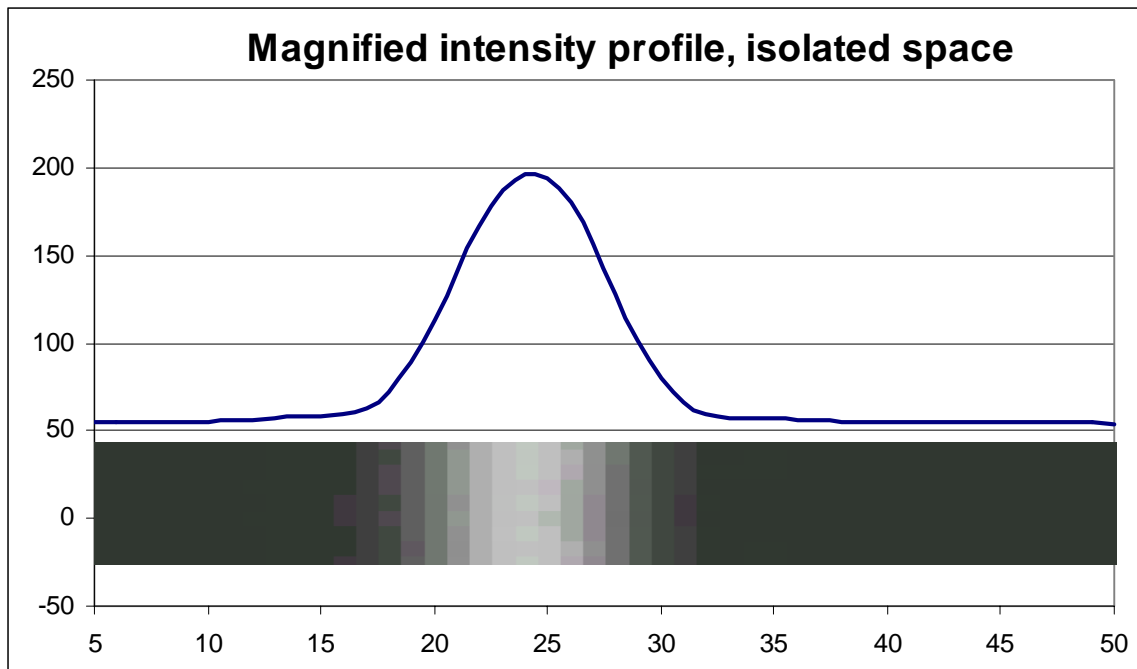


Figure 4. Magnified image and intensity profile for the isolated space from figure 3.

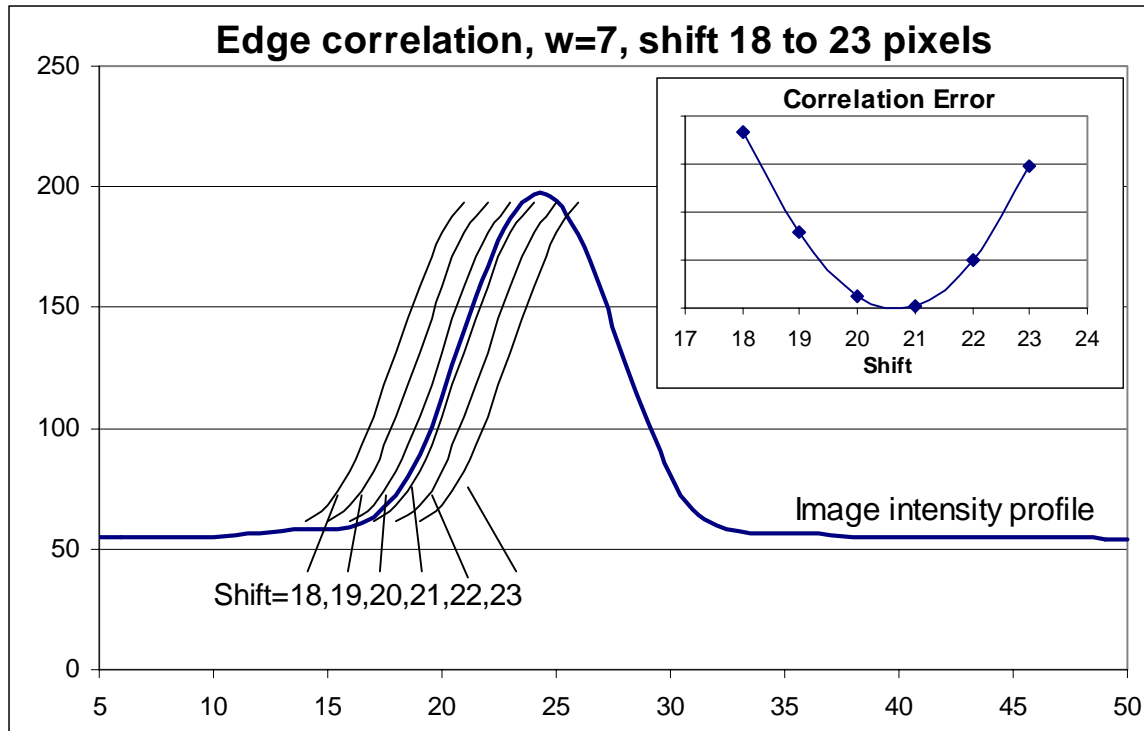


Figure 5. The edge is shifted past the intensity profile and the correlation error is calculated. Here the best match between the edge and the profile is at pixel 20.71.

The results are given in table 1 for the threshold algorithm and the new algorithm for  $w=6$  to  $w=9$ . From the table, if we use the model for a 7 pixel space ( $w=7$ ) we get a final width of 7.40 pixels, and for  $w=8$ , we get 7.29 pixels; the actual width must therefore lie between the models for 7 and 8 pixels. As we don't have profiles between  $w=7$  and  $w=8$ , we fit a curve for the edge positions as a function of model width and solve to get the edge positions consistent with the interpolated model width, in this case the edges are at pixel 20.68 and pixel 28.04 and the width is 7.36 pixels. The difference between the threshold and OPE algorithm is 0.52 pixels or about 17nm.

Model	Edge 1	Edge 2	Width <sub>12</sub>
50% Threshold	20.37	28.25	7.88
W = 6	20.89	28.38	7.50
W = 7	20.71	28.11	7.40
W = 8	20.67	27.96	7.29
W = 9	20.70	27.93	7.23
Final W = 7.36	20.68	28.04	7.36

**Table 1.** Isolated space measurement summary

For isolated features, it is possible to use the whole line model and determine the width directly without determining the edge positions independently. Although this works very well for the isolated features, it has been found not to work well when the feature is placed asymmetrically with respect to adjacent features (the end line in a line/space array for example).

### 2.3 Dense Feature Measurements

To illustrate the algorithm in a more general case, the left hand line of the line/space array shown in figures 6 and 7 will be measured. We need to determine the position of edges 1 and 2 with high precision. As described above, the edge positions will be determined independently and the CD given by the difference in position. By considering the edges independently, the software can measure the distance between any 2 edges allowing pitch and other measurements to be performed.

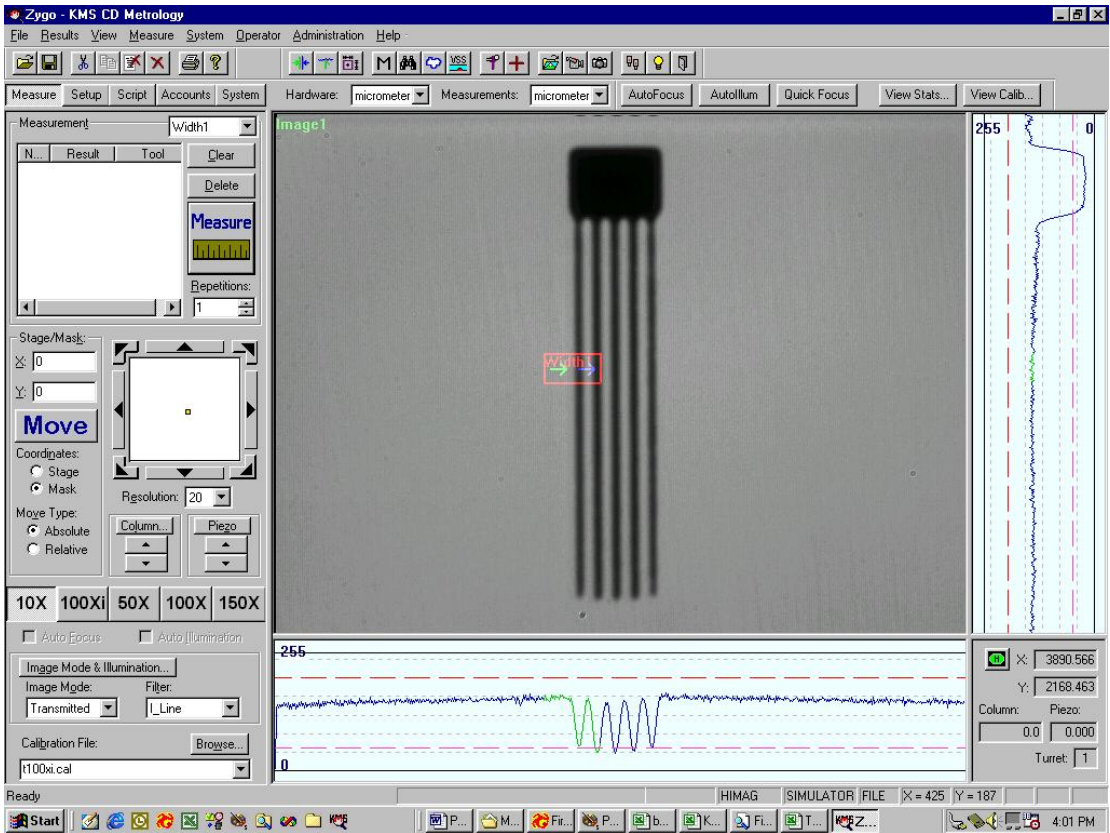


Figure 6. GUI display for the half isolated measurement. We measure the left hand line of the array.

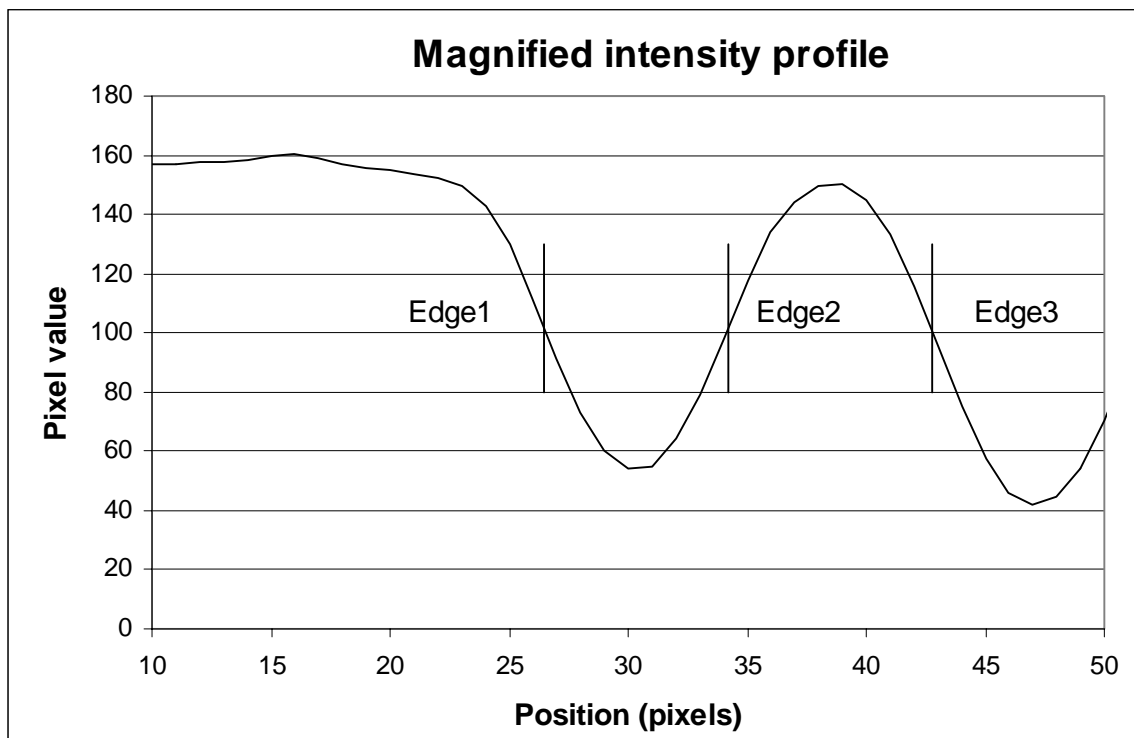


Figure 7. Magnified intensity profile for the half isolated measurement, see figure 6.

The position for the edge 1 proceeds exactly as for the isolated line as described above. For edge 2, we need to consider the left and right adjacent edges (edges 1 and 3). The adjacent edges can be thought to “pull” or “push” the apparent position of an edge, where the strength of the effect will be inversely (or similarly) proportional to the distance from the adjacent edge. We determine edge 2 position by considering the line given by edges 2 and 1 ( $line_{21}$ ) and then by considering the space given by edges 2 and 3 ( $space_{23}$ ), the final position is the compromise between these 2 positions.

The calculation for edge 1 is given in table 2. Edge 1 is determined to be at pixel 26.49.

Model	Edge 1	Edge 2	Line <sub>12</sub>
50% Threshold	26.18	34.24	8.06
W = 7	26.54	34.12	7.58
W = 8	26.48	34.14	7.66
W = 9	26.51	34.10	7.59
W = 10	26.53	34.09	7.56
Final Width = 7.65	<b>26.49</b>	34.14	7.65
<b>Table 2.</b> Edge 1 position calculation.			

The calculation for edge2 is given in table 3, showing the independent calculations based on  $line_{21}$  and  $space_{23}$ .

Model	Edge 2	Edge 1	Line <sub>21</sub>
50%_Threshold	34.24	26.18	8.06
7	34.12	26.54	7.58
8	34.14	26.48	7.66
9	34.10	26.51	7.59
10	34.09	26.53	7.56
7.65	<b>34.14</b>	26.49	7.65
	Edge 2	Edge 3	Space <sub>23</sub>
50%_Threshold	34.24	42.90	8.66
7	34.12	42.99	8.87
8	34.14	42.97	8.83
9	34.10	43.01	8.91
10	34.09	43.02	8.93
8.89	<b>34.11</b>	43.00	8.89
<b>Final</b>	<b>34.13</b>		
<b>Table 3.</b> Edge 2 position calculation			

Using  $line_{21}$ , we get a edge2 position at pixel 34.14 and using  $space_{23}$ , we get edge 2 position at pixel 34.11. The compromise between the 2 calculations is 34.13, biased towards the  $line_{21}$  calculation because edge 1 is 7.65 pixels from edge 2 compared to 8.89 pixels for the distance between edges 2 and 3..

## 2.4 Correlation Error

Mathematically, the match between the model profile and acquired profile is determined by minimizing the error function  $E_n$  for model profile n:

$$E_{w,j} = \sum_i \left( (m_w M_{w,i-j} + b_w) - I_i \right)^2$$

where  $M_w$  are the model profiles as shown in figure 1,  $I_i$  is the intensity profile and  $m_w$  and  $b_w$  are a gain and offset between the model and the intensity profile and are adjusted for each calculation to give the minimum error. By including this gain and offset, we make the algorithm insensitive to the illumination level and any offset in the video signal, we will discuss this further below. The subscript i-j indicates a correlation between the intensity profile and the model, that is, we “slide” the model past the intensity

profile looking for the best fit as indicated by the minimum error. We interpolate between the  $E_{w,j}$  to find the fraction pixel position  $j$ , where we get the best fit.

### 3. RESULTS

The new algorithm has been developed for the new Zygo 244nm DUV CD metrology system, the KMS-100. The results presented are from a prototype KMS-100 and from a production KMS-450 i-line metrology system.

#### 3.1 KMS-100 Optical Platform

The KMS-100 CD metrology system, figure 8, is a new design with the following features:

- Class 10 or better mini-environment.
- Air spaced 0.75NA long working distance objective and 0.7NA condenser for through pellicle metrology.
- Zygo air-cooled 244nm laser.
- Highly stable arch support system.
- 100 $\mu$ m piezo focus.
- Zygo ZMI interferometer stage.



Figure 8 KMS-100 DUV metrology system.

#### 3.2 Static Repeatability

A test mask with isolated clear and dark crosses with nominal sizes from 100nm to 3 $\mu$  was used to evaluate the static repeatability and linearity of the KMS-100. Figure 9 shows the static repeatability results for clear spaces and dark lines as a function of the line width. The results are  $3\sigma$  of 30 measurements taken using a 22 pixel (0.75 $\mu$ ) high box. The pooled  $3\sigma$  for all features, above the design specification of 0.25 $\mu$ , is about 1nm. Below about 0.2 to 0.25 $\mu$  we expect an increase in  $3\sigma$  due to the shape changing less with feature size (below about 100nm, the shape is essentially invariant and the only difference will be the profile size). For the smaller features, there are also fewer pixels to analyze so the effects of noise are also more significant.

#### 3.3 Linearity

Figure 10 shows the deviation from the nominal feature size for the same set of crosses on the KMS-100 compared to results from the KLA-Tencor CD-SEM. The same features were measured although different areas and box sizes were used. We can see that there is no appreciable difference between the KMS-100 measurements and the CD-SEM measurements above 0.25 $\mu$  and even for the smallest feature which is less than 0.2 $\mu$  we get the same delta from the nominal for the KMS and CD-SEM to within a few nm. The only fitting parameter used here was a bias (or line factor) applied to the KMS results. The variation between the KMS and CD-SEM measurements is within the edge roughness of the mask.

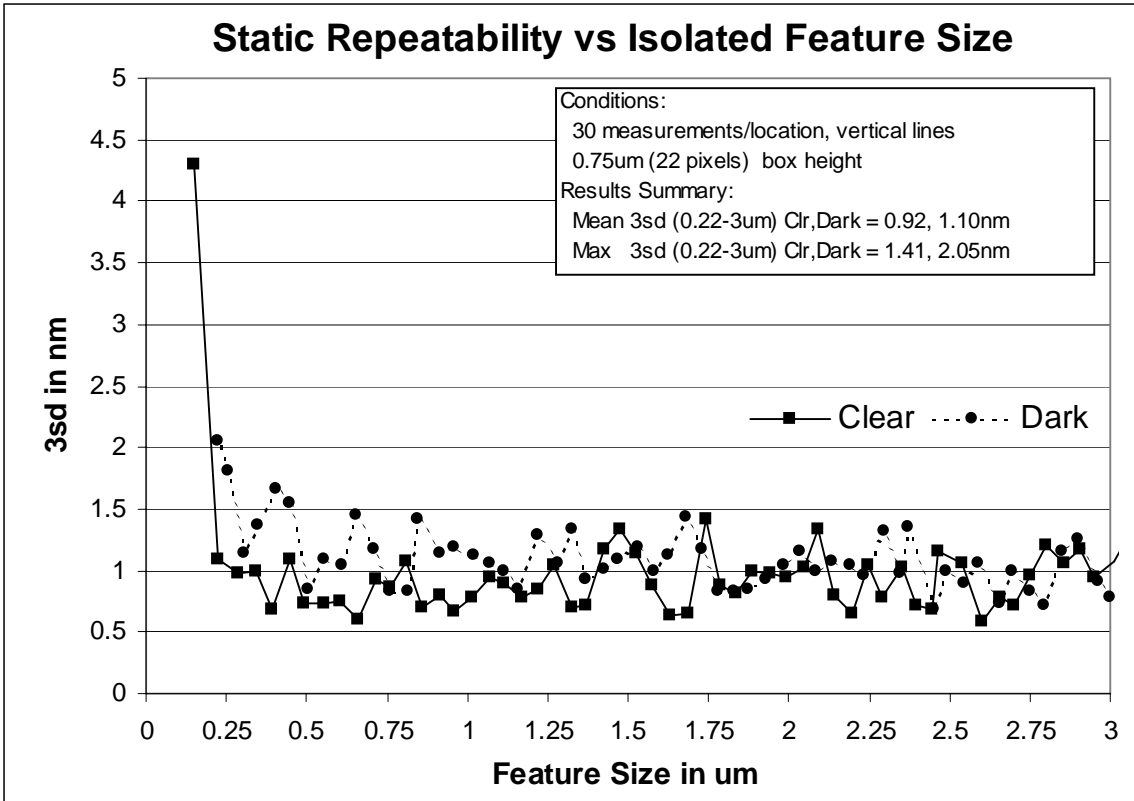


Figure 9. 3σ static repeatability for isolated lines and spaces, 30 measurements per feature using a 0.75μ box.

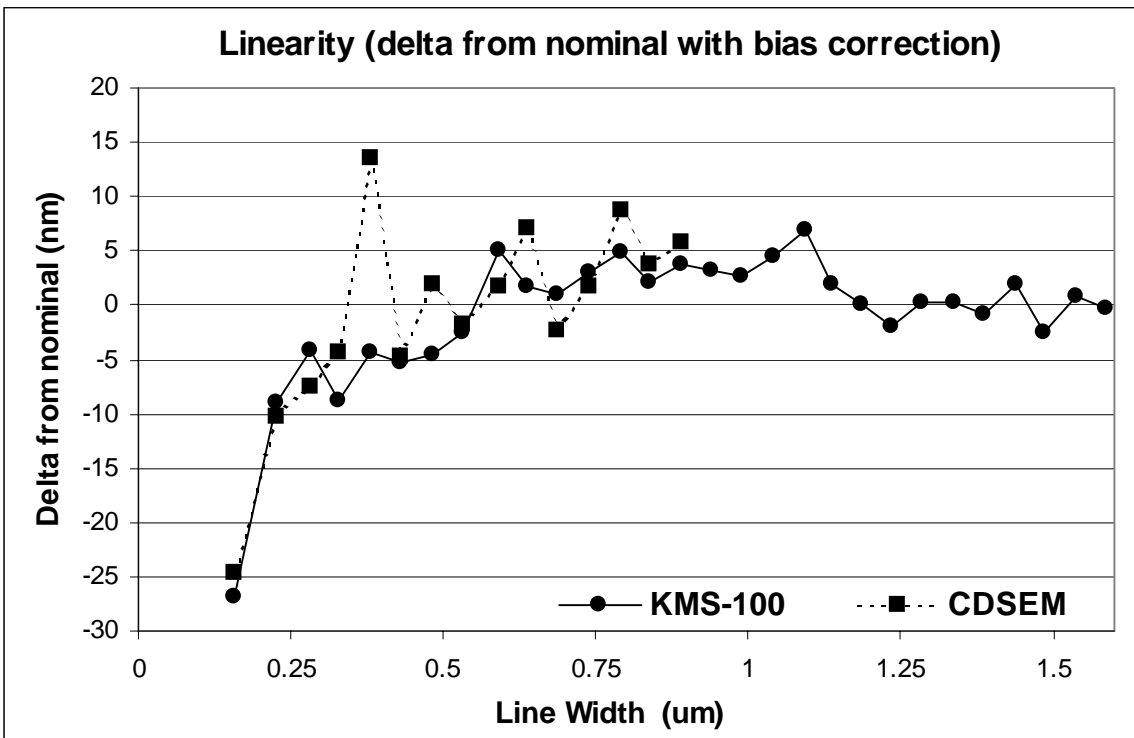


Figure 10. Comparison between the delta from nominal for isolated spaces for the KMS-100 and a CD-SEM.

### 3.4 Isolated/Dense

Figures 11 and 12 show the isolated versus dense performance. Figure 11 shows deviations in measurements of  $0.54\mu$  lines for different aspect ratios in several line space array. In the KMS-450i with the standard threshold algorithm, we get a deviation of about  $40\text{nm}$  when the spacing between lines drops to  $0.26\mu$  (about a 0.5:1 aspect ratio). With the KMS-100 and the new algorithm, we achieve better than  $5\text{nm}$  deviation over the full set of line/space arrays. CD-SEM measurements were used to confirm that the dense and isolated features varied by less than  $5\text{nm}$ .

Figure 12 shows the ability of the new algorithm to measure isolated, dense and “half isolated” lines with little variation. These results were taken on a KMS-450i on a customer’s mask. Each region of the mask was measured a number of times changing the position between measurements, this allows us to get an estimate of the  $3\sigma$  for the measurements and a measure of the variation in feature size. For example, 10 measurements were taken of the top isolated line and we had an average of  $0.427\mu$  and a range of  $5\text{nm}$ . The average values for the different regions varies from  $0.426\mu$  to  $0.430\mu$  for a  $4\text{nm}$  error for isolated, dense and half isolated lines. We would expect at least  $1\text{nm}$  to be due to static repeatability and/or line roughness based on the ranges of measurements at each site.

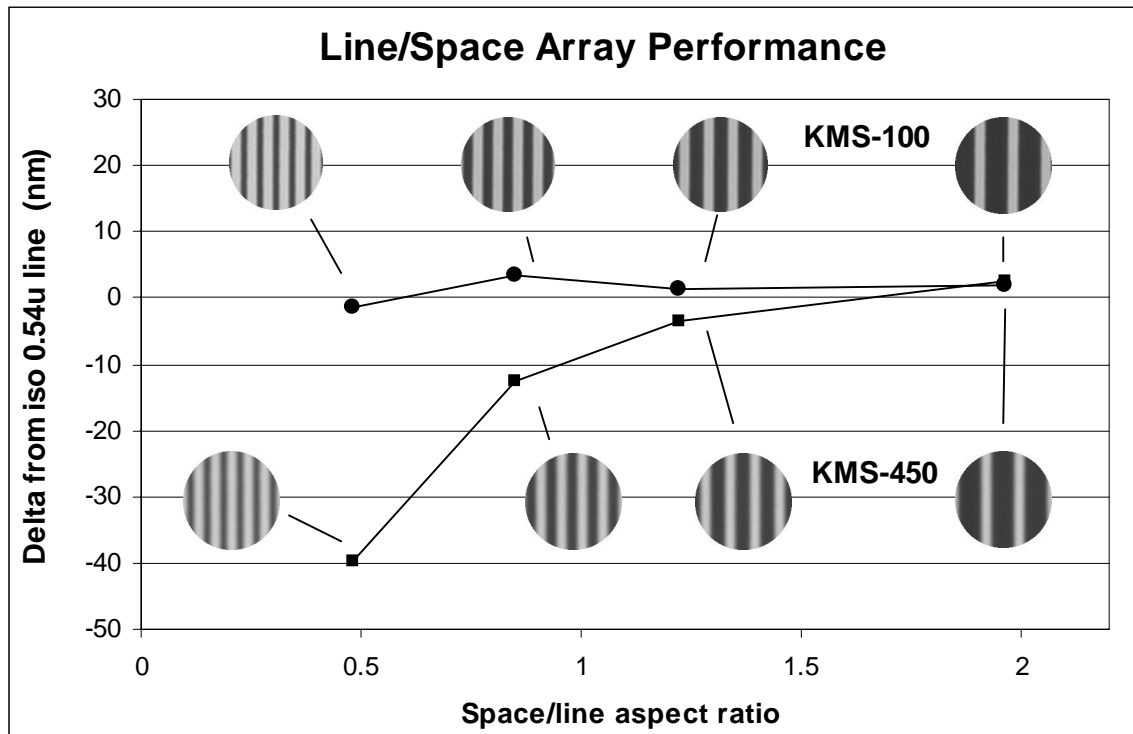


Figure 11. KMS-100 and KMS-450i comparison for dense features in a line/space array. Values are deltas from the  $0.54\mu$  line size.

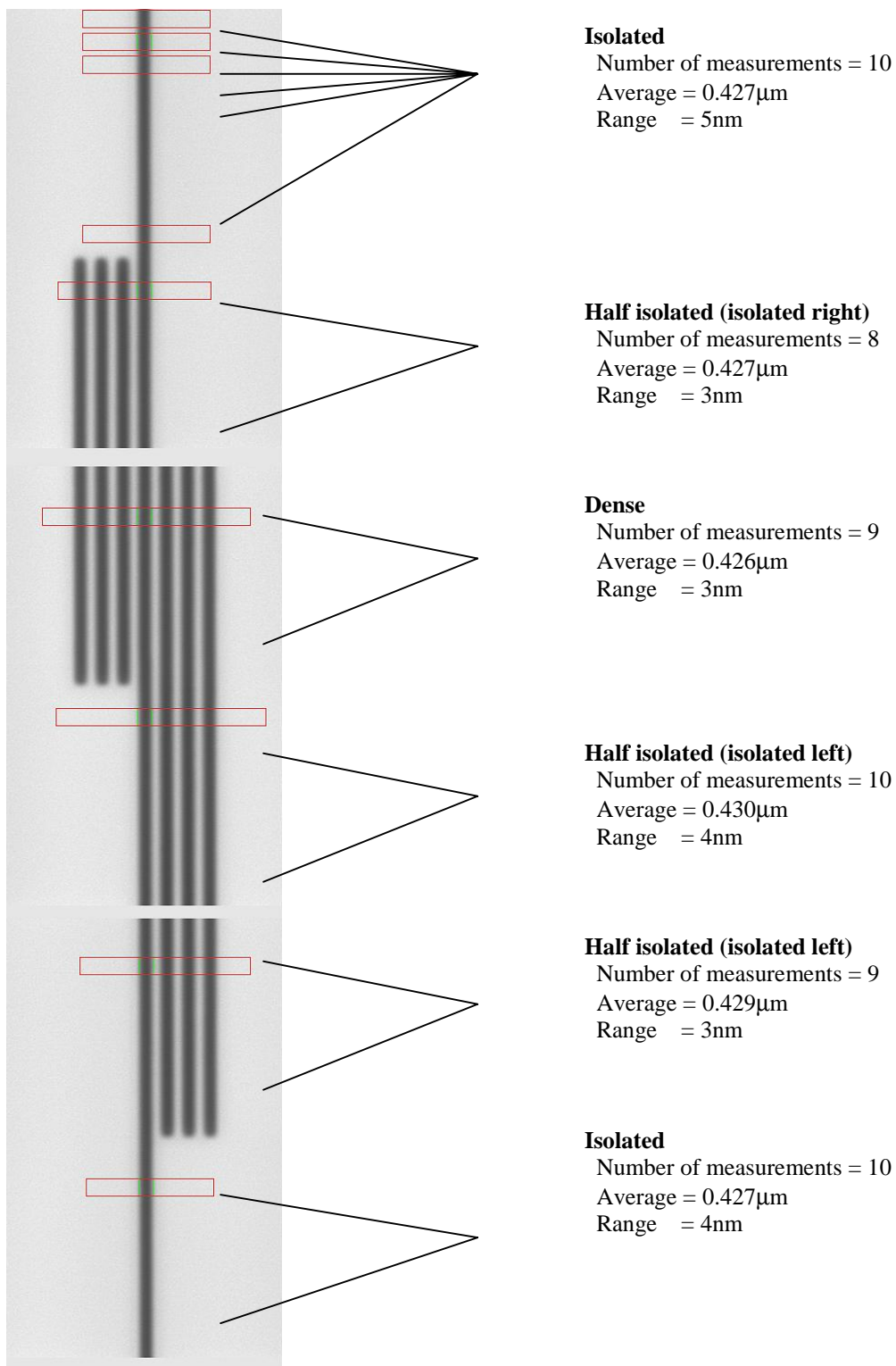


Figure 12. Measurements of isolated, half -isolated and dense KMS-450i results with the OPE algorithm. The average values range from 0.426 $\mu$  to 0.430 $\mu$ .

#### 4. CONCLUSIONS AND DISCUSSION

Much of photomask CD metrology can be thought of in terms of accurate and precise determination of the edges locations of features. Line, space and pitch widths are simply calculated from the differences of edge positions. Edge roughness follows from the analysis of the variation in values along a single edge. Corner rounding calculations can be made on edge coordinates from x and y edge locations, similarly if we find all the edge positions of a shape, its area can be calculated.

We have introduced an edge finding algorithm that makes use of a model of the optical imaging system. The model is implemented by a set of intensity profiles for lines and a set for spaces and the efficacy has been demonstrated for an incoherent imaging system based on the measured MTF. The algorithm makes no assumptions on how the intensity profile data is generated. The mask type and coherence factor etc. will only affect the intensity profiles. We have found that the MTF approach works very well for binary masks and expect good results for attenuated PSM although additional work will probably be needed for strong PSM and resist mask as the assumption that the system is incoherent may not be valid.

It is worth discussing the extension from the isolated to the dense measurement by considering an isolated edge. We can determine the edge position very accurately (in fact we measure an isolated edge for the modeling). Now consider a second edge approaching the first edge (a negative edge approaching from the clear area corresponds to a space whereas a positive edge approaching from the dark area is a line). This second edge will affect the apparent position of the first edge as the "tail" from the second edge interferes with the intensity profile for the first edge. We can think of the second edge as either "pulling" or "pushing" the image of the first edge. The model allows us to correct for this apparent edge shift.

Now if there are 2 adjacent edges, each will push or pull the image of the first edge depending on the distance between the edges. We calculate two apparent positions for the edge based on the adjacent edges and use a compromise between these positions to give us the final position. More work is needed to optimize the form of the compromise calculation.

A combination of the new algorithm and a new optical platform has demonstrated excellent performance in line with the 100nm (now 90nm) node requirements.

#### REFERENCES

1. Goodman, *Introduction To Fourier Optics*, McGraw-Hill, 1996
2. Wilson, Tony, *Scanning Optical Microscopy*, Academic Press, 1984
3. Doe, Nicholas; Eandi, Richard D., "Optical proximity effects in submicron photomask CD metrology" *16th European Conference on Mask Technology for Integrated Circuits and Microcomponents* Uwe F. Behringer, , Proc. SPIE Vol. **3996**, p. 139-154, 2/2000
4. Peter Fiekowsky, Daniel Selassie, "Defect printability measurement on the KLA-351: Correlation to defect sizing using the AVI Metrology System", *SPIE 19th Annual BACUS Symposium on Photomask Technology and Management Conference* **3873**: 7/1999.